

Lattice Dynamics and Dielectric Properties of SiO₂ Stishovite

Changyol Lee

Laboratory of Atomic and Solid State Physics, Cornell University, Ithaca, New York 14853-2501

Xavier Gonze

Unité de Physico-Chimie et de Physique des Matériaux, Université Catholique de Louvain,

B-1348 Louvain-la-Neuve, Belgium

(Received 22 November 1993)

Using the variational density-functional perturbation theory, we compute the phonon band structure, the interatomic force constants, the dielectric tensor, and the Born effective charge tensors of stishovite, a crystalline form of SiO₂ with sixfold coordinated silicon atoms. Comparison with available experimental data shows agreement at the level of a few percent. Access to the real-space interatomic force constants allows us to analyze the interplay between long-range ionic interaction and short-range covalent bonding, as well as criticize available two-body interatomic potentials.

PACS numbers: 63.20.Dj, 61.50.Lt, 77.22.-d

Silica (SiO₂) exists in a surprising variety of polymorphs [1]. There have been abundant experiments [2–4] and theoretical work [5–7] on the structural, dynamical, and electronic properties of silica polymorphs like α - and β -quartz, tridymite, α - and β -cristobalite, coesite, etc., in which the silicon atoms are fourfold coordinated and the oxygen atoms are twofold coordinated. In stishovite, by contrast, silicon atoms are sixfold coordinated, and oxygen atoms are threefold coordinated. Of fundamental interest to geophysics and geochemistry because it is one of the stable high-pressure phases of SiO₂, a major component of the Earth's crust, this form is still incompletely characterized. Experimental problems stem mainly from the smallness of the existing monocrystals which are typically less than 0.3 mm. Phonon frequencies are available only for zone-center modes [3,8–12], and we have been unable to find a study of the low-frequency dielectric tensor. In this context, information from state-of-the-art *ab initio* techniques proves valuable.

In this Letter, we present the results of *ab initio* calculations of the phonon band structure, the real-space interatomic force constants, the high- and low-frequency dielectric tensor, and the Born effective charge tensors of stishovite. We elucidate the interaction between the constituent atoms by a careful analysis of the interatomic force constants and the Born effective charge in the local coordinates whose axes are along and perpendicular to the bond direction.

Our method of calculation is based on the variational density-functional perturbation theory [13,14]. Linear response functions, such as the dielectric tensor, the Born effective charge, and the dynamical matrix [15], are evaluated as second-order derivatives of the total energy, using an expression which is variational with respect to the *first-order* perturbations of the wave functions. The latter quantities are obtained through a self-consistent minimization using a conjugate-gradient algorithm [16] within the local-density approximation (LDA). A detailed description of the method can be found elsewhere [14].

The exchange-correlation expression, as well as pseudopotentials and plane-wave kinetic energy cutoff (30 hartrees), are identical to those used in a previously published study [13]. Convergence of the Brillouin-zone (BZ) integration is studied with grids of 1, 2, 3, 6, and 12 special k points [17].

Stishovite has rutile structure with space group D_{4h}^{14} having Si atoms at $(0,0,0)$ and $(\frac{1}{2}, \frac{1}{2}, \frac{1}{2})$ and O atoms at $(u, u, 0)$, $(1-u, 1-u, 0)$, $(\frac{1}{2}-u, \frac{1}{2}+u, \frac{1}{2})$, and $(\frac{1}{2}+u, \frac{1}{2}-u, \frac{1}{2})$; see Fig. 1. We calculate the equilibrium geometry and the response functions with the different sets of k points given above. For 3 k special points, we find the geometry is well converged (0.001 estimated relative error), as well as the response functions (1% relative error at most). Therefore, results with the 3 k point set are presented in the following. The calculated lattice constants a and c and the calculated internal atomic coordinate u are 4.14 Å, 2.66 Å, and 0.305, respectively, while the corresponding experimental values are 4.18 Å, 2.67 Å, and 0.3062 [18]. Our theoretical lattice constants will be used for further calculations.

The dielectric tensors are calculated in the high- and low-frequency limits. The high-frequency dielectric tensor components along the a and c axes are found to be

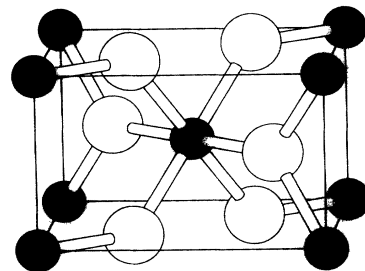


FIG. 1. Unit cell of stishovite. White circles denote O atoms, and dark circles Si atoms. Si atom at the center of the unit cell with 6 O atoms shown make up a SiO_{6/3} octahedron.

TABLE I. Calculated Born effective charge tensors Z_{ij}^* and their principal values ζ_i^* for the Si atom at (0,0,0) and the O atom at ($u,u,0$). The effective charge tensors for other Si and O atoms can be found by symmetry consideration. The components not shown are zero.

Component	Si	O
Z_{xx}^*, Z_{yy}^*	3.803	-1.902
Z_{xy}^*, Z_{yx}^*	0.343	-0.557
Z_{zz}^*	4.055	-2.027
ζ_1^*	4.146	-2.459
ζ_2^*	3.460	-1.345
ζ_3^*	4.055	-2.027

3.31 and 3.50, respectively, with the corresponding experimental values 3.24 and 3.33 [19]. The discrepancy can be attributed to the LDA, which usually underestimates the size of band gaps, as well as to the difficult experimental conditions. Inclusion of the "scissor shift" [20] of 0.17 eV [21] leads to the values of 3.23 and 3.42, respectively. Without local-field corrections (and without the scissor shift), the calculated values are 3.41 and 3.65, respectively. Therefore, local-field effects contribute about 4%. The low-frequency (static) LDA dielectric tensor components, for which no experimental data are available to our knowledge, are 11.01 along the a axis and 9.14 along the c axis. These predicted static dielectric constants are very large compared to the high-frequency ones. For α -quartz, the low- and high-frequency dielectric tensors are different by a factor of about 2. Therefore, the displacement polarizability in stishovite is larger than that in α -quartz.

The Born effective charge tensors Z_{ij}^* are calculated and summarized in Table I. Unlike those of α -quartz [13], the effective charge tensors for both Si and O atoms in stishovite are symmetric. We take the principal axes along and perpendicular to the bond direction to diagonalize the effective charge tensors. We obtain the principal values ζ_i^* of the effective charge tensors, also shown in Table I. Since Si atoms are in a sufficiently symmetric environment, i.e., a center of a $\text{SiO}_{6/3}$ octahedron, their effective charge tensors are nearly isotropic, with principal values differing by 17%. Meanwhile, O atoms have anisotropic effective charge, with principal values differing by 55%.

Next, we present the phonon frequencies at the Γ point. In Table II, we compare the calculated and experimental values for the frequency of each mode at the Γ point. Comparison between this work and the known experimental data gives a rms of absolute deviations of 30.3 cm^{-1} , and a rms of relative deviations of 4.0%. Our results are also similar to theoretical calculations by Vignasina *et al.* [11], while their results have a rms of deviations from experiment of 53.3 cm^{-1} , and 9.3%. The LO-TO splittings are well reproduced except for the A_{2u} splitting. It is not clear that the LO-TO splitting of the A_{2u} mode in Ref. [12] is well established from the experi-

TABLE II. The phonon eigenmodes and the vibrational frequencies of stishovite at Γ . The experimental data are from Ref. [11] for the Raman modes and Ref. [12] for the infrared modes. The frequencies are in cm^{-1} .

Mode	This work	Experiment
	Raman modes	
B_{1g}	214.0	234
E_g	585.4	586
A_{1g}	754.9	751
A_{2g}	599.1	Silent
B_{2g}	954.1	964
	Infrared modes	
B_{1u}	383.6	Silent
E_u (TO)	469.0	470
E_u (LO)	568.9	565
E_u (TO)	595.1	580
E_u (LO)	705.0	700
B_{1u}	761.4	Silent
A_{2u} (TO)	648.8	650
A_{2u} (LO)	1048.5	950
E_u (TO)	821.6	820
E_u (LO)	1043.4	1020

mental point of view because difficulty is reported in the signal-to-noise ratio owing to a small sample size and the region is dominated by the E_u mode. Note that taking the A_{2u} mode frequencies away from the experimental database of phonon frequencies brings down the rms of absolute deviations to 11.0 cm^{-1} and the rms of relative deviations to 2.8%. Experimental values of the LO-TO splittings of the three E_u modes are 95, 120, and 200 cm^{-1} , respectively. The full effective charge tensors predict the corresponding values as 99.9, 109.9, and 221.8 cm^{-1} , while the isotropic parts (traces) of the effective charge tensors $Z^* \delta_{ij}$ with $Z^* = 3.887$ for Si and -1.944 for O atoms predict 119.8, 128.8, and 197.6 cm^{-1} , respectively. Therefore, the LO-TO splittings would be well described by the isotropic parts, unlike the case of α -quartz in which the isotropic parts alone lead to inadequate results. In Table II, one also finds the theoretical values of the three silent modes.

We calculate the real-space interatomic force constants by first subtracting the ionic dipole-dipole interaction, then Fourier transforming the sets of dynamical matrices defined on the Monkhorst-Pack [17] (1, 1, 1), (2, 2, 2), and (2, 2, 4) grids [22]. The long ranged ($1/r^3$) anisotropic dipole-dipole interaction is treated in an analytical way [23] using the Born effective charge tensors previously calculated. The remaining part is effectively short ranged, and we will refer to it as the covalent part. We interpolate the phonon spectra over the whole BZ by inverse Fourier transforming the covalent part of the real-space interatomic force constants, then restoring the dipole-dipole interaction. The interpolated phonon frequencies from the set on the (2, 2, 4) grid show satisfactory agreement, within 2% error, to those from the direct calculations at high-symmetry points in the BZ including Z , X , M , R ,

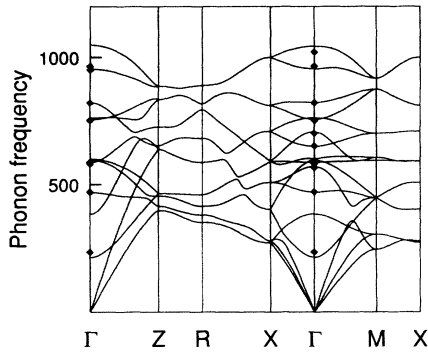


FIG. 2. Phonon spectra of stishovite. The phonon frequencies are in cm^{-1} . Diamonds represent experimental data from Refs. [11] and [12].

and A [24]. In Fig. 2, we show the complete phonon dispersion over the whole BZ. However, as there has been no inelastic neutron scattering experiment for stishovite to our knowledge, we cannot compare the calculated frequencies to experiments except the Γ point. There is no reason for *ab initio* predictions to be less accurate for the entire Brillouin zone than at the Γ point.

The real-space interatomic force constants are useful not only for the interpolation of the phonon dispersion, but because they also give us physical insights in the interaction between atoms.

First, we define "local coordinates" with axes along and perpendicular to the bond direction. The interatomic force constant tensors can be decomposed into the longitudinal and the transverse components with respect to these coordinates. In Table III, we compare the longitudinal components of the interatomic force constant tensors from this work and from two widely used pair potentials for SiO_2 [6,25]. It is easy to establish that interatomic force constants derived from two-body (central) interatomic pair potentials have only longitudinal

components. The discrepancy between the *ab initio* and pair-potential longitudinal force constant is rather large. A measure of the strength (half the spur) of the transverse parts of the interatomic force constant matrix is also provided. These transverse parts are in some cases as important as the longitudinal part. Therefore, we believe that two-body potentials are inadequate for the detailed description of the lattice dynamics of stishovite. A similar conclusion can be reached for α -quartz [23]. Our results clearly advocate the use of three-body potentials.

Each Si atom, at the center of the O octahedron, sees four short (1.75 Å) Si-O bonds and two slightly longer (1.79 Å) Si-O bonds. This environment is clearly different from the one found in tetrahedral SiO_2 polymorphs. From the data in Table III, one finds that the tiny bond length difference (less than 3%) has a drastic effect on longitudinal force constants, and a smaller effect on transverse force constants. One should also notice the very large longitudinal force constants between closest oxygen pairs or between closest silicon pairs. These trends are also observed in the pair potentials. These large force constants can be traced back to dipole-dipole and covalent contributions being of the same sign, while these contributions nearly cancel in the case of Si-O force constants. Note that the covalent parts decrease rapidly with distance, as expected. The decrease of force constants from *ab initio* data is faster than that from pair potentials.

In order to get a quantitative estimate of the range of the covalent interatomic force constants, we calculate the phonon frequencies including covalent forces only for pairs of atoms within some cutoff distance. When this cutoff distance reaches 4.4 Å, we obtain agreement within 2% for the phonon frequencies and within 1% for static dielectric tensors with respect to the calculation without cutoff. This corresponds to the 11th nearest shell of neighbors for Si atoms and the 17th for O atoms.

TABLE III. The longitudinal (C^L) and the transverse (C^T) components of the interatomic force constant tensors (see text). C^L 's are decomposed into dipole-dipole and covalent parts. C^L should be compared with the force constants from pair potentials of Refs. [6] and [25]. Interatomic distances d are in Å and force constants are in $\text{eV}/\text{Å}^2$.

d	C^L	C^T	Dipole-dipole	Covalent	Ref. [6]	Ref. [25]
Si-O						
1.75	-8.0687	4.6101	13.4495	-21.5182	-6.5054	-5.2436
1.79	-4.7579	3.6797	15.1346	-19.8915	-3.7046	-2.2017
3.14	0.9572	0.5593	1.4518	-0.4946	2.9187	3.1714
3.20	1.4412	0.4266	2.3274	-0.8863	2.7416	2.9614
O-O						
2.28	-9.2669	-0.6802	-4.3118	-4.9551	-12.7502	-12.9813
2.50	-3.8784	-0.7973	-1.9999	-1.8785	-8.2750	-8.4713
2.66	-2.2788	-0.8926	-1.9076	-0.3722	-5.9642	-6.1552
3.00	-0.3819	-0.5797	-0.6171	0.2352	-2.9616	-3.1136
Si-Si						
2.66	-8.3525	-0.7881	-7.6305	-0.7220	-8.4433	
3.21	-5.0018	-1.0039	-3.7628	-1.2390	-4.9086	

In conclusion, we have presented a detailed analysis of lattice-dynamical and dielectric properties of stishovite, as obtained using the variational density-functional perturbation theory. The high-frequency dielectric tensor and the phonon frequencies at the Γ point agree at the level of a few percent with experiments. We predict the frequency of three silent phonon modes at Γ , the low-frequency dielectric tensor, the phonon band structure, and the Born effective charge tensors (including their anisotropies). The LO-TO splittings of the phonon frequencies at Γ are well reproduced by either the full anisotropic effective charge tensors or their isotropic parts. The interatomic force constant tensors have also been calculated. The two kinds of Si-O bonds have rather different longitudinal force constants, and less different transverse force constants. The longitudinal force constants between closest Si atoms or closest O atoms are strikingly large, due to dipole-dipole and covalent contributions of the same sign. It is found that the Coulombic and covalent parts of the force constants are comparable and large for the directly bonded atoms, while farther atoms have much smaller covalent parts than the Coulombic parts, as expected. We estimate the range of covalent force constant to be on the order of 4.4 Å. We compare the interatomic force constants derived from widely used two-body interatomic potentials to those derived from our first-principle values and find them rather different.

This work is supported by the Cornell Theory Center and Corning Incorporated (C.L.) and FNRS-Belgium (X.G.). C.L. acknowledges discussions with J. Roth and X.G. thanks D.C. Allan, M.P. Teter, and J.-C. Charlier for their contributions to the development of the density-functional perturbation theory code. The computations were performed on IBM RS-6000 at the Laboratory of Atomic and Solid State Physics, Cornell University.

[1] R. B. Sosman, *The Phases of Silica* (Rutgers University Press, New Brunswick, 1965).

[2] R. W. G. Wyckoff, *Crystal Structures* (Interscience, New York, 1974), 4th ed.

- [3] S. W. Kieffer, *Rev. Geophys. Space Phys.* **17**, 20 (1979).
- [4] G. Wiech, *Solid State Commun.* **52**, 807 (1984); G. Wiech and E. Z. Kurmaev, *J. Phys. C* **18**, 4393 (1985).
- [5] N. R. Keskar and J. R. Chelikowsky, *Phys. Rev. B* **46**, 1 (1992).
- [6] S. Tsuneyuki, M. Tsukada, H. Aoki, and Y. Matsui, *Phys. Rev. Lett.* **61**, 869 (1988); S. Tsuneyuki, H. Aoki, M. Tsukada, and Y. Matsui, *Phys. Rev. Lett.* **64**, 776 (1990).
- [7] Y.-N. Xu and W. Y. Ching, *Phys. Rev. B* **44**, 11048 (1991).
- [8] R. J. P. Lyon, *Nature (London)* **196**, 266 (1962).
- [9] R. J. Hemley, H.-K. Mao, and E. C. T. Chao, *Phys. Chem. Minerals* **13**, 285 (1986).
- [10] A. v. Czarnowski and K. Hübner, *Phys. Status Solidi (b)* **142**, K91 (1987).
- [11] M. F. Vidasina, E. V. Guseva, and R. Yu. Orlov, *Sov. Phys. Solid State* **31**, 747 (1989).
- [12] A. M. Hofmeister, J. Xu, and S. Akimoto, *Am. Mineral.* **75**, 951 (1990).
- [13] X. Gonze, D. C. Allan, and M. P. Teter, *Phys. Rev. Lett.* **68**, 3603 (1992).
- [14] X. Gonze (unpublished).
- [15] S. Baroni, P. Giannozzi, and A. Testa, *Phys. Rev. Lett.* **58**, 1861 (1987).
- [16] M. P. Teter, M. C. Payne, and D. C. Allan, *Phys. Rev. B* **40**, 12255 (1989).
- [17] H. J. Monkhorst and J. D. Pack, *Phys. Rev. B* **13**, 5188 (1976).
- [18] R. J. Hill, M. D. Newton, and G. V. Gibbs, *J. Solid State Chem.* **47**, 185 (1983).
- [19] S. M. Stishov and S. V. Popova, *Geokhimiya* **10**, 837 (1961).
- [20] Z. H. Levine and D. C. Allan, *Phys. Rev. Lett.* **63**, 1719 (1989).
- [21] We use the difference of our calculated band gap to the band gap from the optical studies by Xu and Ching [7].
- [22] P. Giannozzi, S. de Gironcoli, P. Pavone, and S. Baroni, *Phys. Rev. B* **43**, 7231 (1991).
- [23] X. Gonze, J.-C. Charlier, D. C. Allan, and M. P. Teter (unpublished).
- [24] See, for example, M. Lax, *Symmetry Principles in Solid State and Molecular Physics* (Wiley, New York, 1974), p. 446.
- [25] B. W. H. van Beest, G. J. Kramer, and R. A. van Santen, *Phys. Rev. Lett.* **64**, 1955 (1990).

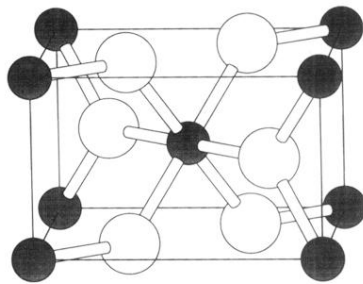


FIG. 1. Unit cell of stishovite. White circles denote O atoms, and dark circles Si atoms. Si atom at the center of the unit cell with 6 O atoms shown make up a $\text{SiO}_{6/3}$ octahedron.